

# Impurity-Helium Solids - Quantum Gels?

V.V. Khmelenko, S.I. Kiselev, and D.M. Lee  
*Laboratory of Atomic and Solid State Physics,  
Cornell University, Ithaca, NY 14853-2501, USA*

C.Y. Lee  
*Hannam University, Taejon, 300-791, Republic of Korea*  
(Dated: April 19, 2002)

Impurity-Helium solids are highly porous van der Waals solids made up of impurity atoms, molecules, or clusters of atoms and molecules surrounded by thin layers of solid helium. The results of structural investigations via ultrasound and X-ray diffraction are reported. Preliminary nuclear magnetic resonance measurements on  $D_2$  impurities in these solids are discussed. Recent electron paramagnetic resonance experiments have explored exchange tunneling reactions in the Impurity-Helium solids. In particular, when D atoms are introduced into an Impurity-Helium solid containing  $H_2$ , the concentration of H atoms is observed to increase, possibly as a result of the reactions  $D + H_2 \rightarrow H + HD$  and  $D + HD \rightarrow H + D_2$ .

PACS numbers: 67.40.Yv, 67.40.Mj, 61.10.Eq, 61.46.+w

## I. INTRODUCTION.

Systems involving impurity atoms or molecules embedded in inert matrices have fascinated physicists and chemists for many years. The demand for high energy rocket fuels in the late 1950's provided an important stimulus to research in this area. A strong program led by the late Herbert P. Broida was established during this period at the National Bureau of Standards (now N.I.S.T.) in Washington, D.C., USA to investigate free radicals trapped in various matrices. Energy storage for long periods of time was made possible by the inert matrices, which served to isolate the individual free radicals from one another, thereby preventing or at least vastly inhibiting chemical recombination. A great deal of emphasis was placed on studies of the free radical atomic nitrogen. The reaction between nitrogen atoms to form nitrogen molecules is the most energetic of all chemical reactions (9.8 eV per  $N_2$  molecule formed). Other free radicals were also investigated including atomic hydrogen. A number of other laboratories became involved in these studies, the results of which were summarized in a book edited by Bass and Broida<sup>1</sup>. Techniques employed included optical spectroscopy, electron spin resonance, thermal measurements and a.c. magnetic susceptibility. Free radicals were created either by gaseous electrical discharges or by X-radiation. The former method was most useful when large free radical concentrations were desired. The contents of the electrical discharge tube were cryopumped into a cold finger cooled externally by liquid helium. The sample consisted of a white, snow-like solid. If nitrogen atoms were present, the sample would emit green light, which corresponded to the decay of a metastable excited state of atomic nitrogen formed in the discharge. In this early work, a number of experiments were performed with nitrogen atoms embedded in a matrix of solid molecular nitrogen. Unfortunately only very low concentrations of atomic nitrogen free radicals

were obtained ( $\leq 0.1\%$ ), far too low for any possible energy storage or rocket fuel applications. Calculations by Jackson<sup>2</sup> performed at the time gave every indication that chain reactions involving recombination would block any attempts to achieve higher concentrations. As time passed, scientists turned to more promising areas of research.

It took more than twenty years for the next major breakthrough to occur in this field. In 1974, E.B. Gordon, L.P. Mezhov-Deglin and O.F. Pugachev<sup>3</sup> in Chernogolovka, Russia invented an entirely new approach to the problem of sample preparation. The basic idea is that gas consisting of a mixture of helium gas and an impurity gas such as atomic and molecular nitrogen was injected into superfluid helium. Much later it was established that a solid formed which was made up of helium and individual impurities or clusters of impurities<sup>4,5</sup>. It is well known that liquid helium solidifies only at pressures of 25 bar or above. The solid formed in the Chernogolovka experiments at the saturated vapor pressure of helium is thought to be composed of the impurity molecules surrounded by layers of solid helium. These solids, known as impurity-helium or Im-He solids, are held together by Van der Waals forces. It is now believed that these solids form porous structures similar to aerogel, where the pores or interstices contain superfluid  $^4\text{He}$ . The "backbone" of these solids consists of the impurities surrounded by thin layers of solid helium. The thin solid helium layers around free radical impurities play a strong role in reducing the recombination rate. The Chernogolovka group also found that when the liquid helium was drained out of the pores, the resulting "dry solid" still maintained its integrity. These new solids have been providing a rich new laboratory for the investigation of atomic or molecular species isolated by helium.

The group at Chernogolovka has been investigating impurity-helium solids for about twenty years. They

have studied solids with rare gas impurities (Ne, Ar, Kr), molecular nitrogen and deuterium impurities, and atomic nitrogen, hydrogen and deuterium impurities. The most powerful methods for studying impurity-helium solids are optical spectroscopy and electron paramagnetic resonance (electron spin resonance or ESR). The former technique has been particularly useful for observing impurity-helium solids containing atomic nitrogen<sup>6,7</sup>. We recall that the early measurements at the National Bureau of Standards observed a green glow emanating for hours from atomic nitrogen radicals trapped in a solid N<sub>2</sub> matrix, for example. The detailed spectrum can provide information on the exact location of the nitrogen atoms relative to the components of the trapping matrix (in this case solid N<sub>2</sub>). In the Chernogolovka experiments, a truly spectacular display resulted when the N-N<sub>2</sub>-He solid was warmed to temperatures well above the normal boiling point of liquid helium. In this case, we are dealing with a dry solid after all the liquid helium has evaporated. As the temperature increases, the diffusion rate of the nitrogen atoms increases. At about 8 K the onset of rapid recombination is manifested by a sequence of bright flashes, indicating that explosive chemical reactions are taking place<sup>8</sup>. Transient spectroscopy could provide considerable detail regarding the kinetics of these explosive events.

Electron spin resonance (ESR) techniques can be used to study any free radical (atomic or otherwise) with an unpaired electron spin. This method is particularly useful for determining the actual free radical content of the sample. The Chernogolovka group performed a series of ESR studies on impurity helium solids containing atomic nitrogen, deuterium and hydrogen impurities<sup>4,9,10</sup>. Inevitably the solids also contained N<sub>2</sub>, D<sub>2</sub> and H<sub>2</sub> molecules, respectively, in addition to the solid helium. As a result of hyperfine interactions and differing nuclear spins and magnetic moments, each of the three atomic species has a unique ESR signature. The Chernogolovka observations revealed that very high concentrations of atomic nitrogen could be stored in the N-N<sub>2</sub>-He impurity helium solids.<sup>4,5</sup> The results were obtained by comparing the observed ESR signal with that of a sample of DPPH with a known number of total spins. It was found that  $[N]/[N_2]$ , the relative concentration of nitrogen atoms, could be as large as 50%. It was therefore possible to obtain total spin densities as high as  $4 \cdot 10^{20}$  per cubic centimeter. The atomic nitrogen concentrations obtained in the impurity-helium solids were orders of magnitude higher than those achieved in the early experiments in the 1950's in the United States and well above Jackson's theoretical prediction. The energy storage was comparable to the best chemical explosives for the highest radical concentrations produced in the impurity-helium solids.

The ESR technique was also applied to a number of other impurity solids at Chernogolovka, including those involving atomic deuterium and/or atomic hydrogen impurities. The most fascinating result was an observa-

tion made on a solid initially containing hydrogen atoms, hydrogen molecules, deuterium atoms and deuterium molecules. It was found that the concentration of hydrogen atoms was considerably larger than the concentration of deuterium atoms in spite of nearly equal concentrations of D<sub>2</sub> and H<sub>2</sub> in the make-up gas<sup>9</sup>. This observation was attributable to the occurrence of chemical reactions in which the hydrogen atom population increased at the expense of a decreasing deuterium atom population.

A program to investigate impurity-helium solids was initiated at Cornell University in early 1998. Prior to this time, one of us (V.V.K.) had been deeply involved in the Chernogolovka research mentioned above. In the 1980's, another of us (D.M.L.) participated in experiments by the Cornell Low Temperature group on spin polarized atomic hydrogen gas, which culminated in the discovery of nuclear spin waves in this rarefied gas<sup>11</sup>. The Cornell research program on impurity-helium solids began with ultrasound studies to obtain information on the structure of these highly porous materials. The results were consistent with an aerogel-like structure. Aerogel permeated with superfluid <sup>3</sup>He or <sup>4</sup>He has been a subject of study at Cornell for many years. This experience was quite valuable in the interpretation of our ultrasound data.

X-ray diffraction experiments performed at the Brookhaven National Laboratory Light Source by our group, as part of a collaboration, provided further information regarding the structure of impurity-helium solids. The aggregation of the impurities into larger clusters was observed in both the X-ray and the ultrasound experiments as the samples were heated above the lambda temperature of liquid helium<sup>12</sup>.

Magnetic resonance studies have been under way at Cornell for the past year. The main results have come from electron paramagnetic resonance studies of nitrogen atoms, deuterium atoms and hydrogen atoms in the impurity helium solids. Some preliminary nuclear magnetic resonance experiments were also performed on an impurity-helium solid containing molecular deuterium.

## II. SAMPLE PREPARATION AND EVOLUTION

The most crucial element required for experiments on impurity-helium solids is the apparatus for sample preparation. The breakthrough by Gordon, Mezhov-Deglin and Pugachev at Chernogolovka has made it possible to collect samples containing copious amounts of free radicals.

In our work we used a variation of the Chernogolovka technique<sup>5</sup>. A schematic diagram of our sample source is shown in fig. 1. A fused quartz capillary is cooled by liquid nitrogen contained in an outer quartz tube concentric with the capillary. Two electrodes placed in the liquid nitrogen each surround the capillary. 60 MHz radiofrequency voltage is applied between the two electrodes when the sample gas is fed through the capillary. The products of the discharge, including any undissoci-

ated molecules, emerge from the bottom of the capillary through a nozzle with a one millimeter diameter orifice. The whole source assembly is surrounded by a double walled stainless steel tube with the region between the inner and outer walls being evacuated to thermally insulate the quartz tubes containing the liquid nitrogen and the sample from the external liquid helium bath region. The lower portion of the assembly is placed in a liquid helium dewar, with the liquid helium level always below the nozzle. Since the sample gas consisted of a mixture of helium and the impurity, it was necessary to prevent freezing out of the impurities in the nozzle, which would give rise to a blockage. This was accomplished by placing an annular heater ( $R \simeq 10\Omega$ ) at the lower end of the capillary. The various gases constituting a sample are stored and mixed in a gas handling system at room temperature (300 K). The sample is then fed into the inner capillary and through the radiofrequency discharge before emerging from the orifice, as discussed above. The sample gas beam is aimed at the center of a small collection beaker a few cm below the orifice. The beaker is kept full of superfluid helium via a fountain pump which transfers liquid to the beaker from the main helium bath whose level is 20 cm below the collection beaker. This compensates for any helium which evaporates during the heating associated with the sample collection procedure. The main bath temperature is held at 1.5 K with the aid of powerful pumps. When the sample is being collected, a small depression appears at the liquid surface just below the nozzle from which the beam emanates. As it exits the nozzle, the beam is clearly visible as a result of light produced from the decay of excited states formed in the discharge. The overall arrangement is shown in fig. 2. As the gas passes through the helium surface, a snow-like solid forms which then sinks to the bottom of the beaker. The "snow flakes" then congeal into a translucent solid corresponding to the impurity-helium solid sample. For the case of a sample containing atomic nitrogen, the solid glows with the characteristic green color seen in the National Bureau of Standards optical spectroscopy experiments. This green light, which persists for several hours, is associated with spectral lines from the decay  $^2D \rightarrow ^4S$  of the metastable states of atomic nitrogen.

In our recent studies, we have been investigating the structure of the porous Impurity-Helium solids by means of ultrasound propagation through liquid helium contained in the pores performed at Cornell University and via X ray diffraction studies conducted at the Brookhaven National Laboratory Light Source. This work is a part of ongoing investigations of Impurity-Helium solids at Cornell University<sup>13,14</sup> and Brookhaven National Laboratory.<sup>12,15</sup> A paper summarizing the collaboration between our group at Cornell and workers at Rutgers, Chernogolovka, and the Max-Planck Institute in Stuttgart is appearing in *Phys. Rev. B* in January 2002.<sup>12</sup> The results of both techniques have indicated that at the formation of the sample at 1.5 K, the impurity entities are either individual impurity atoms or a

few impurity atoms bound together by Van der Waals forces. As the samples warm, diffusion takes place both for helium atoms in the surrounding coatings and for the impurities themselves. The impurity clusters slowly grow in size. This effect is enhanced by release of the heat of aggregation of the impurity clusters which, for the sake of discussion, is taken to be the same order of magnitude as the latent heat of melting of bulk samples of the impurity.

A dramatic increase in the growth rate of the impurity clusters is expected to occur for temperatures above the superfluid transition  $T_\lambda$  because the thermal conductance of liquid helium in the pores becomes dramatically smaller as the sample is heated through  $T_\lambda$ . Thus the heat of aggregation can lead to local hot spots which contribute to higher diffusion rates in these localized regions, a situation which is favorable to the formation of larger impurity clusters. It is therefore to be expected from this crude model that heating the sample above  $T_\lambda$  and then cooling back through  $T_\lambda$  would lead to irreversible behavior. As we shall see, this is exactly what has been observed in the most recent experiments. The expected time evolution according to this model for a sample is shown in fig. 3.

For the case of atomic free radical impurities, the very large amount of heat released during molecular recombination enhances the effects described above. It was found that for very high concentrations of free radicals, the sample would spontaneously explode. In the following section we present ultrasound data and X-ray diffraction data from our experiments. These recent results are consistent with the qualitative description discussed above.

### III. ULTRASOUND AND X-RAY DATA.

We shall first discuss the ultrasound experiments performed by the Cornell group. The impurity helium sample was formed in a sound cell (shown in fig. 4 which consisted of a pair of quartz (1 MHz fundamental) or lithium niobate crystal transducers separated by a distance of 1.5 cm. The sound cell was placed in the collection beaker. Transparent deflecting shields were placed above the cell to channel the Im-He solids into the sound propagation path. The transducers were often operated at the odd harmonics 3 MHz and 5 MHz. A pulse-time-of-flight method was used to measure the velocity and the attenuation of the sound as it traversed the sample, which consisted of a porous aerogel-like solid with the pores being filled with liquid helium. The sound propagated mainly through the liquid helium in the pores as evidenced by the fact that the sound velocity was very close to that of bulk liquid helium. The attenuation of sound on the other hand, was greatly influenced by the presence of the porous impurity-helium sample. The attenuation results were indeed dependent on the history of the sample, as expected from the qualitative model presented previously.

The next set of figures illustrates this point. Figure 5 portrays sound attenuation results for Kr-He, Ne-He, N<sub>2</sub>-He and D<sub>2</sub>-He impurity-helium solids. The sequence of events during the warm up of a sample involves successive decoupling of the normal fluid component from the walls of successively smaller channels as the viscous penetration depth decreases with increasing temperature according to  $\delta_{visc} = (2\eta/\omega\rho_n)^{1/2}$ . Here  $\eta$  is the viscosity,  $\omega$  is the angular frequency of the sound and  $\rho_n$  is the normal fluid density which increases with temperature according to the two-fluid model. This increased freedom for the normal fluid to flow dissipatively as the temperature rises leads to a concomitant increase in the sound attenuation as shown in fig. 5. A plateau is eventually reached where sound propagates mainly through the largest channels, a process which can be thought of as sound propagation through bulk liquid helium.

It is noteworthy that the samples containing heavier impurities tend to have a considerably higher sound attenuation, ranging from the lightest solid sample D<sub>2</sub>-He with an attenuation close to that of bulk liquid helium to the heaviest, Kr-He which has the highest attenuation. For the case of the D<sub>2</sub>-He solid, a possible interpretation is that the D<sub>2</sub>-He solid has almost the same density as that of bulk superfluid helium, so that sound propagation will be relatively unimpeded due to the close matching of the acoustic impedances. The acoustic impedance becomes more mismatched with increasing impurity mass, leading to higher attenuation.

Figure 6 illustrates the history dependence of the sound attenuation as the impurity-helium samples are heated and then cooled. If the heat is applied until the sample is warmed above the lambda temperature, an irreversible change takes place which is manifested by a considerably higher attenuation as the sample is cooled below the lambda temperature. If the sample was heated to a point just below the lambda temperature and then cooled down the attenuation behaves reversibly. We believe that these results show that larger clusters of impurities are formed at temperatures above the lambda point as described in our qualitative picture. These larger (and therefore heavier and denser) impurity clusters give rise to a larger attenuation as shown in fig. 6, where data for N<sub>2</sub>-He samples, D<sub>2</sub>-He samples and D<sub>2</sub>-He samples containing atomic deuterium are represented. This latter sample exhibits an even higher attenuation increase after heating and cooling through the lambda point as a result of additional heat generated via recombination of deuterium atoms into D<sub>2</sub> molecules.

The ultrasound experiments also furnish information on the characteristic pore size in these porous impurity helium solids, where we point out that the pore sizes actually extend over a range of values, in analogy with light aerogels. The key parameter needed to describe the behavior of sound attenuation in liquid <sup>4</sup>He in porous materials is the viscous penetration depth. In superfluid helium, the normal fluid fraction changes from nearly zero to unity between 1.0 K and 2.17 K, causing  $\delta_{visc}$  to

change from 1500 nm to 100 nm for 5 MHz sound. As a sample of superfluid <sup>4</sup>He contained in the pores of our impurity helium solid is cooled, the viscous penetration depth increases, so more and more of the fluid is locked to the walls. Therefore, at the lowest temperature, where almost complete locking occurs, dissipative sloshing of the normal fluid through the pores is minimal. The attenuation thus decreases as the sample is cooled. This effect is quite evident for temperatures below a crossover temperature of about 1.5 K (depending on sample and sound frequency). Above this temperature, the attenuation is so large that sound propagates relatively freely only in the very largest (macroscopic) channels where bulk helium behavior is observed, corresponding to a saturation of the attenuation above the crossover temperature. By calculating the viscous penetration depth at this temperature, we can find the corresponding pore size which for our samples ranges from 200-800 nm. The very smallest pores were studied by observing the attenuation at  $T_\lambda$ . The smallest pores were about 8 nm. This type of analysis plus the fact that the sound velocities are always nearly equal to that for bulk liquid helium provides very convincing evidence that we are dealing with highly porous materials. A more complete discussion of these effects is given in papers by Kiselev *et al.*<sup>12,14</sup>

Information obtained from the x-ray measurements<sup>12</sup> were consistent with the ultrasound results. The impurity-helium solids were placed in the path of the synchrotron radiation x-ray beam at the Brookhaven National Laboratory light source. Experiments were performed with 17.3 keV x-rays (beam line X20B) for Ne-He samples and with 8 keV x-rays (beam line X20A) for all other samples. Figure 7 shows a diagram of the variable temperature x-ray cryostat insert used in these experiments. The samples were contained in a beryllium can which was lowered into the path of the x-ray beam. Since the impurity-helium samples were random in nature, powder pattern diffraction peaks were measured. Broad diffraction peaks correspond to very small clusters whereas narrow diffraction peaks correspond to larger nanocrystallites, since more crystal planes are available to scatter the incident x-rays, giving rise to sharper diffraction patterns. The action of diffusion in the impurity-helium solids is expected to lead to the formation of larger crystallites. Immediately following the preparation of impurity-helium samples, cluster peaks were not observed, in almost all cases. Only for the case of Ne-He samples was a very broad neon cluster peak observed upon formation of a Ne-He solid sample. As the sample was heated above the lambda temperature the neon cluster peaks became higher and narrower, exactly as one would expect when larger crystallites formed as a result of diffusion. The diffraction angles of the observed peaks corresponded to peaks expected for solid neon. Figure 8 shows a set of peaks corresponding to different temperatures as the Ne-He sample was warmed from 2.5 K to 4.2 K. The sample was always surrounded by liquid helium for this set of measurements.

For the other impurity-helium solids, the results can be described as follows: After heating the Im-He samples up to 4 K, broad impurity cluster peaks were observed for D<sub>2</sub>-He, N<sub>2</sub>-He and the mixed sample D<sub>2</sub>-N<sub>2</sub>-He. Evaporating liquid helium from the cell led to the creation of relatively large impurity microcrystallites. Diffraction peaks corresponding to these larger crystallites became higher and narrower as the temperature increased above 4 K in these "dry" solids. As discussed above, the larger crystallite sizes corresponded to smaller widths as is normally the case in x-ray diffraction. A careful analysis is discussed in ref. 12. Typical sizes ranged from 30 Å to 80 Å.

Finally, fig. 9 shows a N<sub>2</sub>-He impurity solid result in which the sample was always surrounded by liquid helium. The lower trace gives the signal at 1.5 K before warming to 4 K. The signal is indistinguishable from that of the helium background which has not been subtracted. After heating the sample to 4 K and cooling it back to 1.5 K a broad nitrogen peak was observed, as indicated by the upper trace. This result again illustrates the growth of nanocrystallites as a result of warming the sample through the lambda temperature.

Two different types of measurements, ultrasound and x ray studies, have shown that diffusion gives rise to the formation of tiny crystallites of the impurity as samples of impurity-helium solids are warmed up through the lambda temperature of liquid helium. Further experiments and theoretical studies are required to progress from the qualitative ideas presented herein to a quantitative understanding. The importance of this work is that it shows quite clearly the necessity of maintaining the impurity-helium solids at temperatures below the lambda temperature to prevent excessive recombination for the free radical impurities and structural changes in all samples. This is especially significant for purposes of any applications requiring energy storage.

#### IV. NMR STUDIES OF IMPURITY-HELIUM SOLIDS

Nuclear magnetic resonance (NMR) is an extremely versatile technique which permits measurements of spin diffusion and relaxation processes, mainly by means of pulse methods. It should be primarily useful in studies of H<sub>2</sub> and D<sub>2</sub> molecules in the impurity helium solids. The technique suffers from the disadvantage that nuclear moments are rather small. This, combined with the dilution of spins found in impurity helium solids leads to the expectation that serious signal to noise problems might be encountered. The problem is further exacerbated in H<sub>2</sub> samples because of the Pake doublet splitting associated with the intramolecular dipole-dipole interaction in the J=1 orthohydrogen. This kind of interaction is a much more manageable problem in the case of deuterium for which the nuclear dipole moment is about one sixth that of hydrogen.

In our experiments, success was finally achieved in a deuterium-helium impurity solid studied by means of a CW resonance spectrometer operating at 3.66 MHz with lock-in detection. The only way signals could be obtained was by increasing the ratio of deuterium to helium in the make up gas. Make up gas for this sample consisted of D<sub>2</sub>:He in ratio 1:10. No signal was observed shortly after the initial formation of the D<sub>2</sub> helium solid. It was only possible to see a signal when the sample was heated well above the lambda temperature of liquid helium (see fig. 10). We concluded that it was necessary to form small crystallites before a signal could be observed. The lack of a response at the lowest temperatures is perhaps attributable to saturation with the longitudinal relaxation time being too long for isolated deuterium molecules immediately following sample preparation. This saturation becomes a much less serious problem as small crystallites of solid deuterium form in the sample as a result of diffusion at the higher temperatures. Nevertheless, in spite of our best efforts, we were never able to achieve satisfactory signal to noise ratios to perform reliable quantitative measurements.

We are forced to the conclusion, on the basis of these experiments, that NMR experiments in these impurity helium solids must be carried out at much higher fields to provide enhancement of the signal to noise ratio as a result of a more favorable Boltzmann factor and higher sensitivity.

#### V. ELECTRON SPIN RESONANCE STUDIES OF IMPURITY-HELIUM SOLIDS

An important set of electron spin resonance (ESR) studies was carried out at Chernogolovka on impurity helium solids.<sup>5,9,10</sup> At our laboratory at Cornell, we have recently begun to investigate the ESR spectra of the nitrogen impurity-helium solid and solids involving atomic hydrogen and atomic deuterium impurities. Since the electronic moments are quite large, in contrast with nuclear moments, very large signals can be observed as a result of the large transition frequencies associated with spin flips, and the correspondingly large Boltzmann factors. Thus it is possible to investigate small, dilute samples. If the steady magnetic field is sufficiently homogeneous, ESR lines corresponding to transitions between various hyperfine states can easily be resolved. For the case of high spin densities, however, the dipole-dipole interaction can lead to enough line broadening to prevent resolution of the hyperfine lines.

In our experiments at Cornell, we have employed a continuous wave (CW) 9.07 GHz microwave homodyne spectrometer. An electromagnet provided a homogeneous steady field H<sub>0</sub> up to 10 kG. The homogeneity ( $\Delta H/H < \sim 10^{-5}$ ) was determined via the nuclear magnetic resonance signal from a water sample. A cylindrical TE<sub>011</sub> resonant cavity (see fig.11) operating in the reflection mode was positioned in our metal cryostat near the

midpoint of the magnet pole pieces. The cylindrical axis of the cavity was aligned vertically. A hole through the center of the top of the cavity allowed the sample to be inserted. The central position of this hole ensured that the sample would be placed in the maximum microwave magnetic field  $H_1$ . The hole had a minimum effect on the operation of the cavity, since the electric field at this position was minimized for the  $TE_{011}$  mode. Microwaves were generated by a klystron and then routed to the cavity by a circulator. The signal reflected from the cavity was sent by the circulator to the receiver which consisted of detectors and an amplifier chain. The magnetic field at the position of the cavity was modulated by a pair of coils attached to either side of the cavity. The coils generated a 100 kHz alternating magnetic field. Data was taken as the magnetic field of the large electromagnet was swept slowly through the ESR lines. The modulation field was kept small enough to produce an undistorted derivative of the ESR signals, but large enough to provide an adequate signal level. The signal leaving the detector was dominated by the modulation frequency. This signal was amplified and then fed into a lock-in amplifier which greatly enhanced the signal to noise ratio. The output of the lock-in detector was displayed on a chart recorder trace and was also recorded in a computer to allow for rapid data processing. The actual spectral lines were obtained by integration of the derivative signals obtained in this way.

A small ruby crystal, mounted inside the resonant cavity, provided a comparison signal to help calibrate the amplitude of the sample signal. The sample and the ruby are expected to vary in the same way as the temperature fluctuates or the spectrometer sensitivity drifts. The ruby can in turn be calibrated against a known sample of DPPH to enable us to determine the absolute number of spins in our samples. The ESR lines of ruby are highly dependent on the orientation of the crystal. An orientation was chosen so that the ruby signals did not overlap the signals produced by samples.

The microwave power entered and exited the resonant cavity through a small 50  $\Omega$  coaxial cable connected to a small coupling loop constructed from a single turn of Cu wire. At the top of the cryostat, the coaxial cable was connected to the X-band wave guides of the bridge. Typically 5 microwatts of microwave power were delivered to the resonant cavity. The cable lengths were tuned so that the output of the circulator was significant only when an ESR line was being traversed as the field of the electromagnet was varied. The impurity-helium samples were formed in a special beaker which consisted of a small quartz tube closed off at the bottom. A quartz funnel was attached to the top of the tube to collect the sample which is created at the top of the cell. A pair of rotating teflon blades was employed to sweep any of the impurity-helium solid that might have stuck to the funnel into the lower portion of the sample tube.<sup>10</sup>

During the collection procedure the sample cell beaker was placed high in the cryostat, just underneath the ori-

fice. The beaker was kept full of liquid helium by the fountain pump, as discussed earlier. The sample cell was then lowered into the main superfluid bath and then into its final position with the tube corresponding to the lower end of the cell positioned inside the resonant cavity.

The atoms being studied in our ESR investigations are nitrogen, deuterium and hydrogen. The value of  $H_0$  employed in these experiments places us close to the high field regime of the Breit-Rabi formula. Therefore a small shift of the observed spectra from the high field limit is expected and is seen in the data. The simplest spectrum is obtained for hydrogen atoms because the proton and the electron are each spin 1/2 objects. This leads to four possible spin states. The selection rules for magnetic dipole transitions give two hyperfine lines in the ESR spectrum of hydrogen. The large proton moment leads to a very large splitting (508 G) between these lines. The deuterium ESR spectrum has three lines, almost equally spaced (the departure from equal spacing corresponds to the value of  $H_0$  being slightly below the high field limit). The triplet structure comes about as a consequence of the deuterium spin being  $I=1$ . The deuteron magnetic moment is smaller than that of the proton so that the splitting between components of the triplet (76.7 G and 78.7 G) is smaller than the hyperfine splitting for the case of the atomic hydrogen doublet. Atomic nitrogen also has three hyperfine lines in its ESR spectrum. The nitrogen splitting (4.2 G) is more than an order of magnitude smaller than that for deuterium. Hence for the case of impurity helium solids with high nitrogen atom concentrations the line broadening associated with the dipole-dipole interactions makes it more difficult to resolve the individual hyperfine lines.

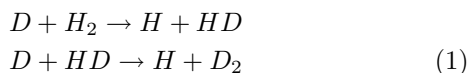
Preliminary ESR measurements were performed on atomic nitrogen in a N-N<sub>2</sub>-He impurity helium solid. In fig. 12, we show the derivative signal for ESR lines obtained for an impurity helium solid with a moderate relative concentration of nitrogen atoms. The characteristic triplet structure is present, but the three individual lines are not well separated. Better resolution was obtained when more dilute samples were measured. The nitrogen results were very similar to those obtained at Chernogolovka at a much earlier date<sup>4,5</sup>. These measurements were used mainly to develop our experimental procedures, since it is much easier to obtain very large free radical concentrations for atomic nitrogen.

The main subject of our most recent investigations has been the study of impurity helium solids containing hydrogen and/or deuterium atoms. Three well resolved deuterium peaks were observed in all the solids containing deuterium atoms. Figure 13 shows the derivative signals for an impurity helium solid with only deuterium impurities (deuterium atoms and molecules). The deuterium atom population was observed to decay very slowly at 1.3 K. This is attributable to recombination. When the sample was heated to 4.2 K the signal dropped quickly as rapid recombination occurred. The latter result is in agreement with previous work at

Chernogolovka<sup>10</sup>.

Investigations involving atomic hydrogen in impurity helium solids can only be performed when there are heavier impurities along with the hydrogen. The reason for this is that a solid mixture of hydrogen and helium is typically less dense than liquid helium and hence will float to the surface. An impurity solid containing neon impurity atoms as well as the hydrogen atoms was prepared. A doublet corresponding to the ESR signal for hydrogen atoms was found. The hydrogen atom population decayed exponentially with a time constant  $\tau$  of about 80 minutes in this solid as a result of H atom recombination.

We have recently obtained new results in impurity helium solids containing H, D, H<sub>2</sub>, and D<sub>2</sub>. Early results at Chernogolovka showed that these mixed solids were formed with larger than expected concentrations of hydrogen compared with deuterium<sup>9</sup>. They hypothesized that exchange tunneling reactions were occurring in which D atoms substituted for H atoms in molecular H<sub>2</sub> thus producing free atomic hydrogen. Quantum diffusion processes were expected to bring the reactants into contact. The actual reaction sequence was thought to be as follows:



Ivliev *et al.*<sup>17</sup> studied these reactions in a solid consisting of H atoms and D atoms in a solid matrix consisting of H<sub>2</sub> and D<sub>2</sub>. They again observed that isotope exchange reactions corresponding to those mentioned above were occurring. They were actually able to observe the increase of the H atom ESR signal and the decay of the D atom ESR signal as time progressed. Their experiments were performed at 4.25-5.3 K where they showed that quantum diffusion was required for these reactions to proceed.<sup>17</sup> Parallel investigations were made on these dilute H and D systems in solid H<sub>2</sub> by Miyazaki *et al.*<sup>18</sup>

In our ESR experiments, we were able to monitor the changes in population of H atoms and D atoms as a function of time in H, D, H<sub>2</sub>, D<sub>2</sub> mixed impurity helium solids. Experiments were performed for various make up gas mixtures containing different proportions of H<sub>2</sub> and

D<sub>2</sub>. The results were very sensitive to these ratios.

A typical set of traces illustrating the evolution of the hydrogen doublet and the deuterium triplet derivative signals is given in fig. 14 for a 1:8 ratio of H<sub>2</sub>:D<sub>2</sub> in the make up gas used to prepare the sample. The basic time dependence of the signals is entirely consistent with the occurrence of exchange tunneling reactions with the H atom content increasing with time.

For a make up gas ratio H<sub>2</sub>:D<sub>2</sub> of 1:2, the signal associated with the D atoms declined exponentially with time constant  $\tau=230$  min, whereas the H signal declined slowly with a linear time dependence. When the ratio of the make up gas H<sub>2</sub>:D<sub>2</sub> was changed to 1:4, even more dramatic behavior was revealed. For this case the D signal declined exponentially just as for the case of the 1:2 mixture but the H signal increased with the passage of time. Similar behavior was seen in a 1:8 mixture as portrayed in fig. 15. In fig. 15, we show plots of the time evolution for the 1:8 mixture, which gives a more detailed time dependence of the reaction kinetics. It is to be noted that these observations were made at 1.37 K so that the reactions were driven by quantum tunneling. The observed behavior is entirely analogous to that observed by Ivliev *et al.*<sup>17</sup> and Miyazaki *et al.*<sup>18</sup> on H and D in a matrix of solid H<sub>2</sub>, but the concentrations were far greater in our experiments. Thus in our experiments we have investigated the kinetics of the tunneling exchange reactions in a regime where very high concentrations were available. In future studies we intend to investigate the possibility of producing H atom concentrations of 10<sup>18</sup> atoms per cm<sup>3</sup>. The thermal de Broglie wave length is comparable to the mean interatomic spacing at about 30 mK for this concentration. If the recombinational heat is not too high, we might be able to achieve low enough temperatures such that dramatic quantum effects may be observed.

## VI. ACKNOWLEDGEMENTS

The authors wish to thank NASA for supporting this work via NASA grant NAG 8-1445.

<sup>1</sup> A.M. Bass and H.P. Broida, "Formation and Trapping of Free Radicals" (Academic Press, New York 1960)

<sup>2</sup> J.L. Jackson, *Formation and Trapping of Free Radicals*, edited by A.M. Bass and H.P. Broida (Academic Press, New York and London, 1960), p. 327

<sup>3</sup> E.B. Gordon, L.P. Mezhev-Deglin, O.F. Pugachev, JETP Lett. **19**, 63 (1974)

<sup>4</sup> E.B. Gordon, V.V. Khmelenko, E.A. Popov, A.A. Pelmenov, O.F. Pugachev, Chem. Phys. Lett. **155**, 301 (1989)

<sup>5</sup> E.B. Gordon, V.V. Khmelenko, A.A. Pelmenov, E.A.

Popov, O.F. Pugachev, A.F. Shestakov, Chem. Phys. **170**, 411 (1993)

<sup>6</sup> R.E. Boltnev, E.B. Gordon, V.V. Khmelenko, I.N. Krushinskaya, M.V. Martynenko, A.A. Pelmenov, E.A. Popov, A.F. Shestakov, Chem. Phys. **189**, 367 (1994)

<sup>7</sup> R.E. Boltnev, E.B. Gordon, V.V. Khmelenko, M.V. Martynenko, A.A. Pelmenov, E.A. Popov, A.F. Shestakov, *J. de Chimie Physique* **92**, 362 (1995)

<sup>8</sup> R.E. Boltnev, I.N. Krushinskaya, A.A. Pelmenov, D.Yu. Stolyarov, V.V. Khmelenko, Chem. Phys. Lett. **305**, 217 (1999)

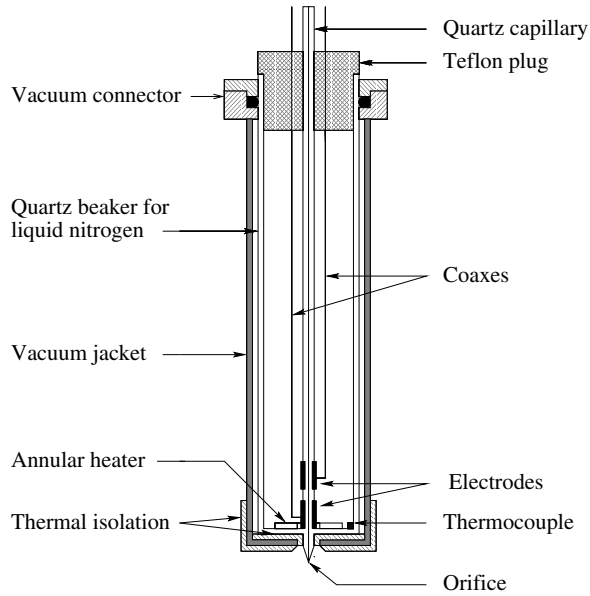


FIG. 1: Diagram of the source of atoms and molecules used for preparation of Im-He solids.

- <sup>9</sup> E.B. Gordon, A.A. Pelmenev, O.F. Pugachev, and V.V. Khmelenko, *JETP Lett.* **37**, 282 (1983)
- <sup>10</sup> E.B. Gordon, A.A. Pelmenev, O.F. Pugachev, V.V. Khmelenko *Sov. J. Low Temp. Phys.* **11**, 307 (1985)
- <sup>11</sup> B.R. Johnson, J.S. Denker, N. Bigelow, L.P. Levy, J.H. Freed, and D.M. Lee, *Phys. Rev. Lett.* **52**, 1508 (1984); N.P. Bigelow, J.H. Freed, and D.M. Lee, *Phys. Rev. Lett.* **63**, 1609 (1989)
- <sup>12</sup> S.I. Kiselev, V.V. Khmelenko, D.M. Lee, V. Kiryukhin, R.E. Boltnev, E.B. Gordon, and B. Keimer, *Phys. Rev. B* **65**, 024517-1 (2002)
- <sup>13</sup> S.I. Kiselev, V.V. Khmelenko, D.A. Geller, J.R. Beamish, and D.M. Lee, *J. Low Temp. Phys.* **119**, 357 (2000)
- <sup>14</sup> S.I. Kiselev, V.V. Khmelenko, and D.M. Lee, *Low Temp. Phys.* **26**, 641 (2000)
- <sup>15</sup> V. Kiryukhin, B. Keimer, R.E. Boltnev, V.V. Khmelenko, E.B. Gordon, *Phys. Rev. Lett.* **79**, 1774 (1997)
- <sup>16</sup> S.I. Kiselev, V.V. Khmelenko, D.M. Lee, V. Kiryukhin, R.E. Boltnev, E.B. Gordon, and B. Keimer, *J. Low Temp. Phys.* **126** (2002) (to be published)
- <sup>17</sup> A.V. Ivliev *et al.*, *JETP Lett.* **38**, 379 (1983)
- <sup>18</sup> H. Tsuruta, T. Miyazaki, K. Fueki, N. Azuma, *J. Chem. Phys.* **87**, 5422 (1983); T. Miyazaki, K.-P. Lee, K. Fueki, and A. Takeuchi, *J. Chem. Phys.* **88**, 88 (1984); T. Miyazaki, N. Iwata, K.-P. Lee, K. Fueki, *J. Chem. Phys.* **93**, 3352 (1989),

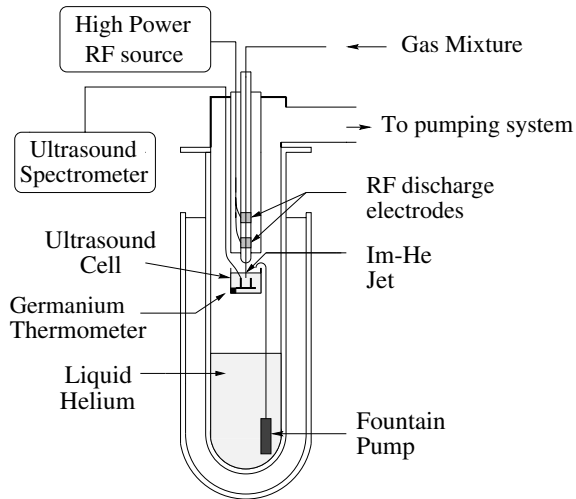


FIG. 2: Experimental setup for preparation of Impurity-Helium solid samples for ultrasound studies.

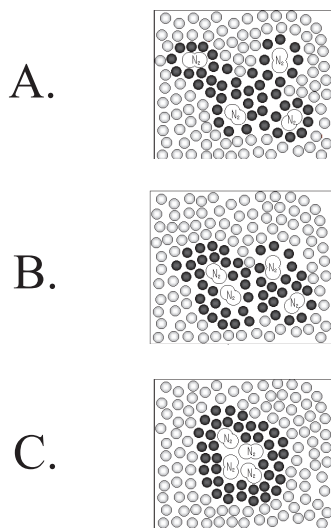


FIG. 3: The model of Im-He solid formation: A. On formation, the impurities are mainly isolated from one another by helium atoms in the solid (black circles). Superfluid liquid helium contained in the pores (gray circles) transports heat efficiently. B. As the sample is warmed up, diffusion allows impurities to aggregate slowly. The associated heat is carried away by superfluid helium. C. As the sample is warmed above the  $T_\lambda$ , the diffusion rate increases. Larger aggregates form. The heat of aggregation can no longer be carried away by liquid helium for  $T > T_\lambda$ . More diffusion takes place and even larger aggregates form.

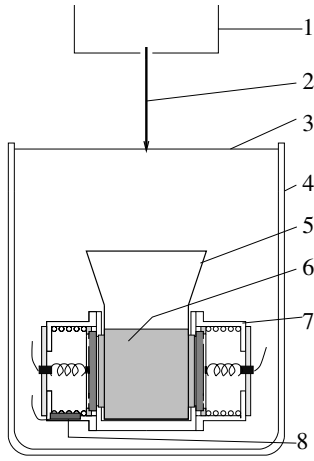


FIG. 4: Ultrasound cell.

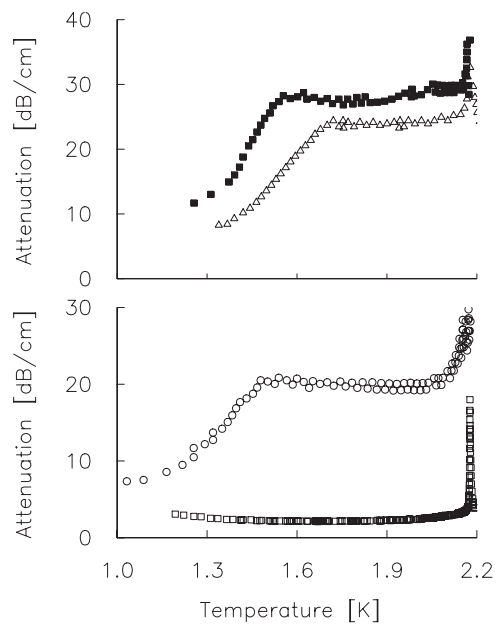


FIG. 5: The behavior of ultrasound attenuation in liquid helium confined in different impurity-helium solids: (a) in Kr-He solid (solid squares), in Ne-He solid (triangles); (b) in N<sub>2</sub>-He solid (open circles), in D<sub>2</sub>-He solid (open squares).

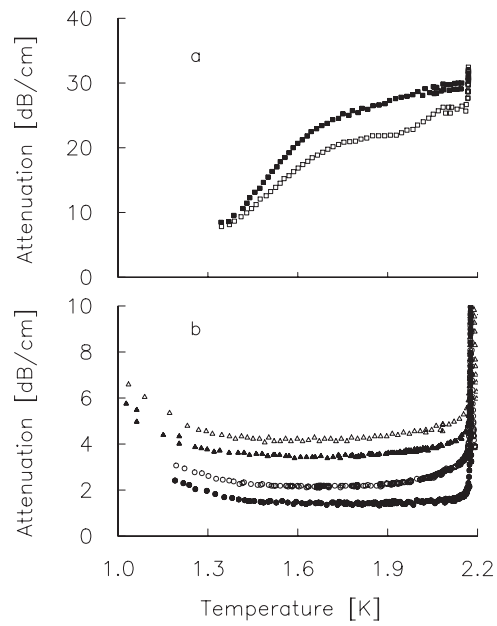


FIG. 6: The attenuation of ultrasound in liquid helium: (a) in N<sub>2</sub>-He solids [after preparation (open squares), after crossing  $\lambda$ -point and cooling down (solid squares)]; (b) in bulk helium (solid circles), in D<sub>2</sub>-He and D-D<sub>2</sub>-He solids [after preparation of both solids (open circles)], after crossing  $\lambda$ -point and cooling down D<sub>2</sub>-He (solid triangles), after crossing  $\lambda$ -point and cooling down D-D<sub>2</sub>-He (open triangles).

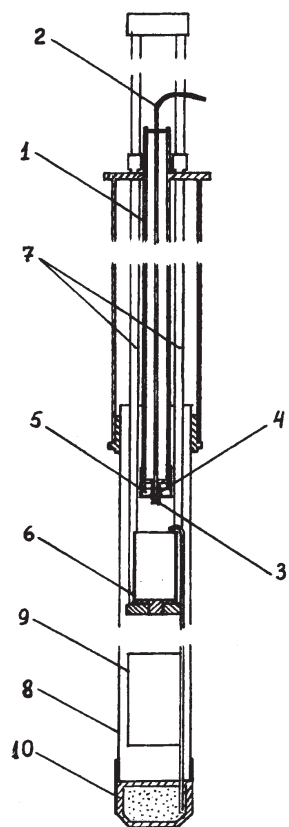


FIG. 7: Diagram of the insert for a variable temperature Oxford cryostat. The access hole for the x-rays also allows entry of liquid He from the main bath.

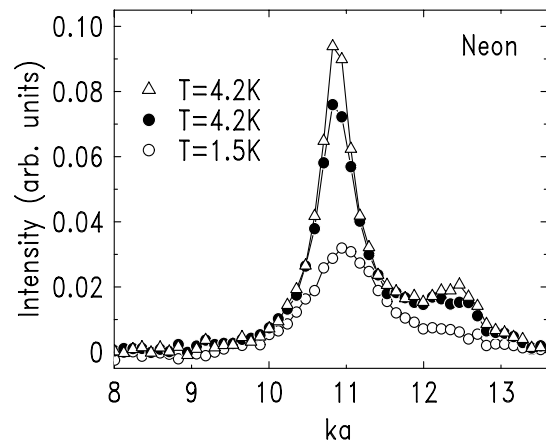


FIG. 8: X-ray diffraction patterns for the Ne-He samples immersed in liquid helium at  $T=1.5$  K and  $T=4.2$  K. Liquid helium signal is subtracted.  $k$  is momentum transfer,  $a$  is the lattice constant of solid Ne. The lower curve at  $T=4.2$  K was taken immediately after the sample was warmed up. The higher curve at  $T=4.2$  K was taken 15 min afterwards.<sup>12</sup>

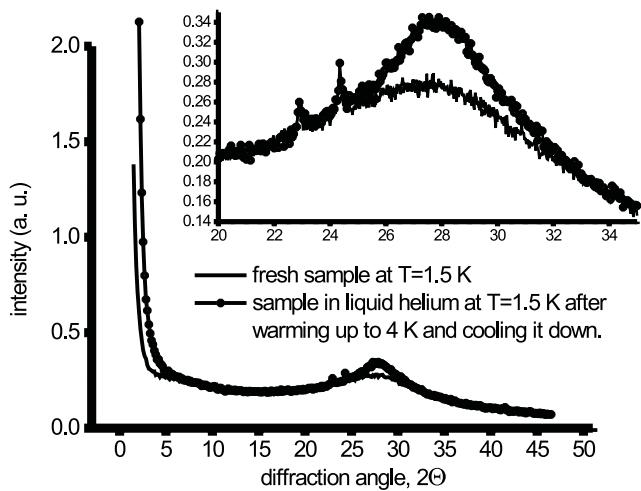


FIG. 9: X-ray diffraction pattern ( $E=8\text{keV}$ ) from  $\text{N}_2\text{-He}$  solid immersed in liquid helium, where helium background is included. The inset shows the signal on a finer scale.<sup>16</sup>

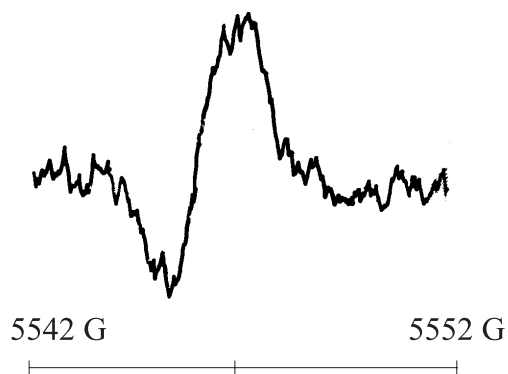


FIG. 10: NMR signal from  $D_2$ -He solid after it was heated well above  $T_\lambda$  and cooled down to  $T=1.5K$  ( $f=3.66$  MHz).

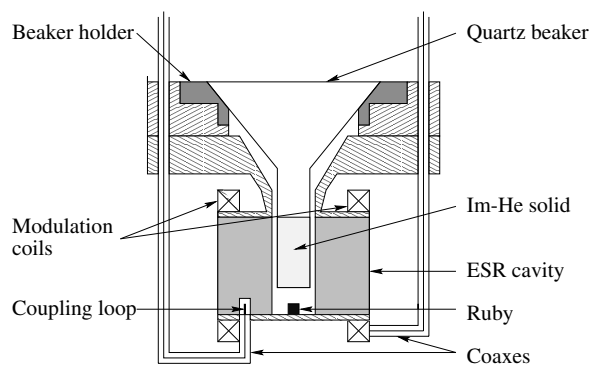


FIG. 11: Diagram of the ESR cell used in these experiments, showing the sample container and the  $TE_{011}$  resonant cavity operating at 9.07 GHz.

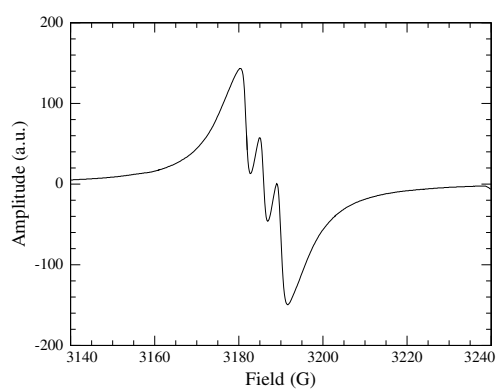


FIG. 12: ESR spectrum of nitrogen atoms in  $N_2$ -He solid ( $f=9.07$  GHz) at  $T=1.43K$ . The poor resolution results from the dipole-dipole interaction between the N atoms.

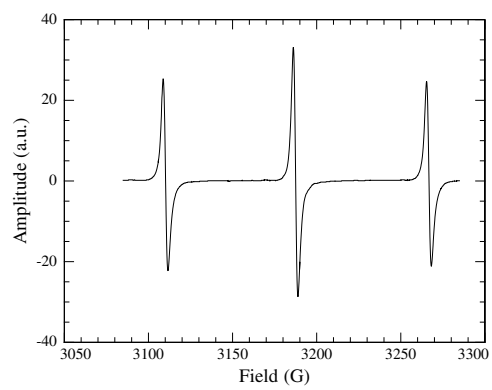


FIG. 13: ESR spectrum of D atoms in  $D_2$ -He solids at  $T=1.38K$  ( $f=9.07$  GHz).

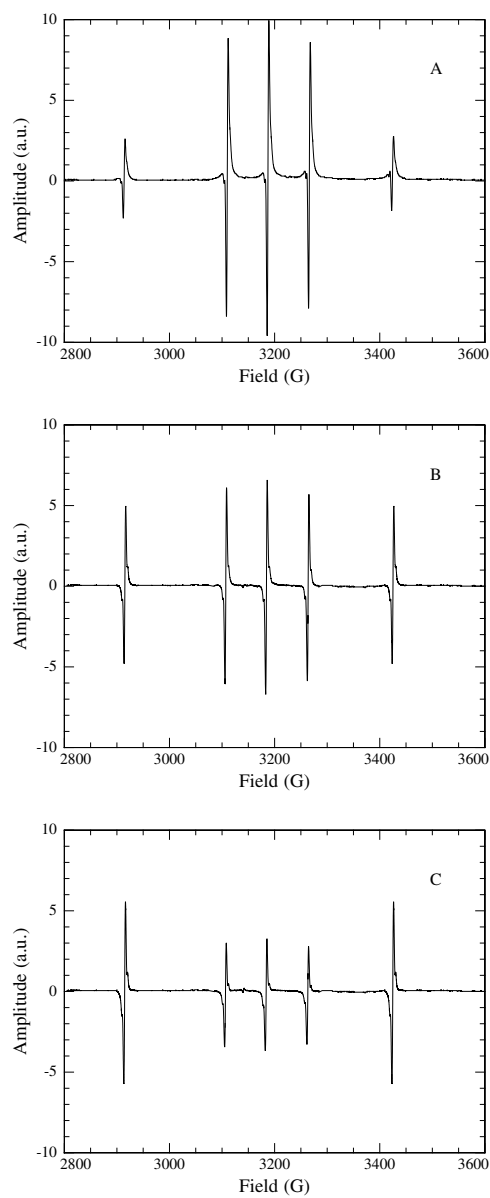


FIG. 14: ESR spectra from H atoms (doublet) and D atoms (triplet) in  $\text{H}_2\text{-D}_2\text{-He}$  solid taken at  $T=1.37\text{K}$  at: a)  $t=23$  min, b)  $t=205$  min, and c)  $t=479$  min after sample collection. ( $\text{H}_2\text{:D}_2\text{:He}=1\text{:}8\text{:}180$ )

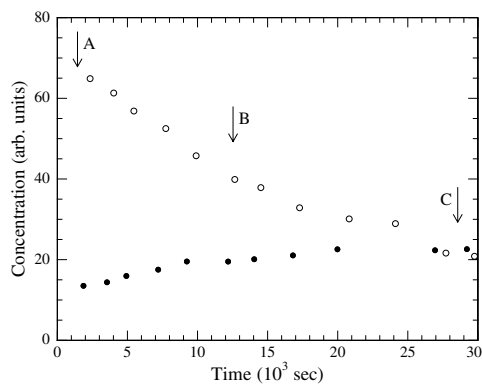


FIG. 15: Time dependence of concentrations of H atoms (closed circles) and D atoms (open circles) in H<sub>2</sub>-D<sub>2</sub>-He solid (H<sub>2</sub>-D<sub>2</sub>-He=1:8:180). The arrows indicate the times at which ESR spectra presented on fig.14 were taken.